Communication

Leaky-Wave Antenna Array With a Power-Recycling Feeding Network for Radiation Efficiency Improvement

Yunjie Geng, Junhong Wang, Yujian Li, Zheng Li, Meie Chen, and Zhan Zhang

***Abstract*— A novel kind of leaky-wave antenna (LWA) array with a power-recycling feeding network is proposed for radiation efficiency improvement. The antenna array is constructed by two kinds of substrate-integrated waveguide LWAs with different periodic slots. One kind of the LWA is designed to work on the fundamental ($m = 0$) wave and radiates in the forward direction. The other one is designed to work on the -1th ($m = -1$) spatial harmonic and radiates in the backward direction. The nonradiated power at the end of one kind of the LWA is directly fed into the other (adjacent) kind of the LWA in reverse direction. Therefore, the reversed feeding can compensate the opposite radiation direction of the two kinds of LWAs, and result in a superposition of radiation. So, both the gain and radiation efficiency of the antenna can be significantly improved, while the array maintains a compact size as those of traditional planar arrays. Simulation results are compared with measurement results to validate the proposed concept of integrating different leaky-wave structures into one array.**

***Index Terms*— Antenna arrays, leaky-wave antennas (LWAs), power-recycling, radiation efficiency, substrate-integrated waveguide (SIW).**

I. Introduction

Leaky-wave antennas (LWAs), which work on traveling-wave, are known as high directivity, frequency scanning capability, and simplicity of feeding network [1]. However, this kind of antennas are usually terminated with matching load to avoid reflections, so only one part of the input power leaks out, and the radiation efficiency is low. As we know, when the length of leaky wave antenna increases, more power will leak out, and the radiation efficiency will be improved, but this is not a practical approach in most applications because of the limitation of antenna size.

Recently, several types of LWAs using power-recycling network to improve radiation efficiency were proposed. Reference [2] used a rat-race coupler to connect the input and output ports of the LWA, so that the power at the end of the structure can be recycled back into the antenna input port again to increase the overall efficiency. Reference [3] proposed a high-efficiency LWA array, which recycled the power at the output port of the center element back into the input ports of the neighboring elements. Using these two approaches, the radiation efficiency of the LWAs has been significantly improved. However, the operating principle and design procedure of the first antenna proposed in [2] are relatively complex, and the power-recycling feeding network structure of the second antenna proposed in [3] is not compact due to the additional power divider and cables between the adjacent elements.

Manuscript received September 25, 2016; revised February 3, 2017; accepted March 3, 2017. Date of publication March 15, 2017; date of current version May 3, 2017. This work was supported in part by the National Nature Science Foundation of China under Grant 61331002 and in part by the National Program on Key Basic Research Project under Grant 2013CB328903.

The authors are with the Key Laboratory of All Optical Network and Advanced Telecommunication Network of Ministry of Education, China, and also with the Institute of Lightwave Technology, Beijing Jiaotong University, Beijing 100044, China (e-mail: 15111009@bjtu.edu.cn).

Color versions of one or more of the figures in this communication are available online at http://ieeexplore.ieee.org.

Digital Object Identifier 10.1109/TAP.2017.2681322

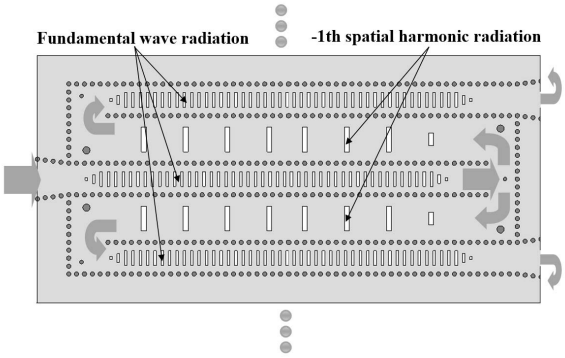

Fig. 1. Basic principle of the antenna array with a power-recycling feeding network.

In this communication, we present a novel solution to improve the radiation efficiency of LWAs by using hybrid radiation of fundamental wave and -1th spatial harmonic of the leaky waveguide. Using this method, the radiation efficiency, as well as the gain, of leaky wave antenna is improved significantly, while the antenna structure remains compact. The antenna is designed on substrate-integrated waveguide (SIW) [4]–[6] structure, which has the desirable features from both the traditional rectangular waveguide and the printed antennas [15]–[18], such as high-Q factor, high-power capacity, low cost, low profile, and easy integration with planar circuits.

This communication is organized as following. Section II discusses the theory of the periodically slotted LWAs used in this communication. Section III gives a detailed procedure of the antenna design. Section IV shows the fabricated structures and experimental results. Finally, conclusions are given in Section V.

II. Theory and Formulas

Fig. 1 gives the schematic of the antenna structure. Two kinds of LWA structures with different periods of slots are designed compactly on the same SIW substrate, and form a planar antenna array. The signal is fed into the central element first. The rest power at output port of the central element is divided into two parts, and reversely fed into the adjacent two elements directly. At the output ports of the elements other than the central one, the rest power is directly fed into the next unfed elements. So, the waves traveling in adjacent elements are in opposite directions. The adjacent two LWA elements are designed to work on fundamental ($m = 0$) wave and -1th ($m = -1$) spatial harmonic, respectively. As we know, the fundamental wave is radiating in the forward direction, while the -1th spatial harmonic is radiating in the backward direction. Therefore, this opposition of radiation directions can compensate the opposition of traveling wave directions in adjacent elements. By properly selecting the parameters of the antenna structure, we can finally realize the objective that all the elements radiate in the same direction.

Since the periodically slotted SIW LWAs have similar properties as those of periodically slotted rectangular waveguides, so in theory, the

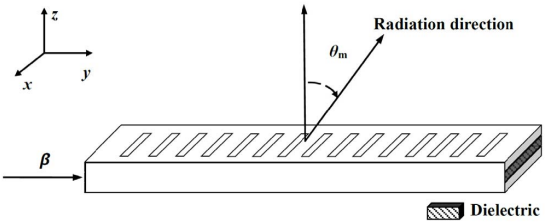

Fig. 2. Configuration of the leaky rectangular waveguide with periodic slots.

antennas are analyzed based on the periodically slotted rectangular waveguides [7], [8]. For a leaky rectangular waveguide with periodic slots cut in the top wall, as shown in Fig. 2, the guided wavelength can be expressed as

$$\lambda_g = \lambda_0/\sqrt{\varepsilon_g} \tag{1}$$

where, ε_g is an equivalent dielectric constant of the leaky waveguide, and is expressed by

$$\varepsilon_g = \varepsilon_r - (\lambda_0/\lambda_c')^2. \tag{2}$$

Here, ε_r is the dielectric constant of the material filled in the waveguide, and it equals to 1 when there is no dielectric; λ_0 is the wavelength in free space, and λ_c' is the cut off wavelength of the fundamental mode in the leaky waveguide. For the rectangular waveguide, the fundamental mode is TE_{10}. λ_c' is actually different from that in the closed waveguide, but the difference is not significant. The propagation constant of the leaky waveguide is then expressed by

$$\beta = k_0\sqrt{\varepsilon_g} \tag{3}$$

where k_0 is the wave number in free space.

As we know, periodic structures can generate infinite spatial harmonics, and only those with smaller (than free space) propagation constant can leak away from the structures. The radiation condition and beam angle of the mth harmonic are

$$-1 < \sqrt{\varepsilon_g} + m\lambda_0/P < 1 \tag{4}$$

$$\theta_m = \sin^{-1}(\sqrt{\varepsilon_g} + m\lambda_0/P) \tag{5}$$

where P is the period of slots.

From the analysis, we find that the radiation beam directions of the spatial harmonics of leaky waveguide are determined by both the equivalent dielectric constant ε_g and the period of slots P, so either changing ε_g or changing P will lead to changing radiation beam angle. It can also be found that for a leaky waveguide, when $\varepsilon_g < 1$, both the harmonics with negative order ($m < 0$) and positive order ($m \geq 0$) can generate leaky waves. But when $\varepsilon_g \geq 1$, only those harmonics with negative order can generate leaky wave, which is similar to that of leaky coaxial cable. In our design, we combine two kinds of periodic slots structures, corresponding to radiation of fundamental ($m = 0$) wave and -1th ($m = -1$) spatial harmonic, respectively, to form a 2-D antenna array, as shown in Fig. 1.

For the design of fundamental wave radiation antenna, $\varepsilon_g < 1$ must be satisfied. From formula (2), a relatively smaller cut off wavelength, corresponding to a smaller width of the waveguide, is needed. Besides $\varepsilon_g < 1$, all the higher order harmonics must be suppressed, which can be done by selecting relatively smaller period of slots according to (4). For the design of -1th spatial harmonic radiation antenna, $\varepsilon_g > 1$ must be satisfied, so a larger width of the waveguide must be selected to obtain a larger cut off wavelength of the waveguide. Besides $\varepsilon_g > 1$, higher order harmonics other than $m = -1$ must be suppressed for single-beam radiation. According to (4), the slots period P should meet the condition

$$\lambda_0/(\sqrt{\varepsilon_g} + 1) < P < 2\lambda_0/(\sqrt{\varepsilon_g} + 1). \tag{6}$$

When the LWA structure for fundamental wave radiation is determined by the given beam angle θ_0 and formulas (1)–(5), the LWA structure for -1th spatial harmonic radiation should be designed according to

$$\theta_{-1} = -\theta_0 \tag{7}$$

and formulas (5) and (6). Therefore, when the two kinds of LWAs are integrated, on the same substrate, into a planar array as shown in Fig. 1, the radiation beams of all the elements will point to the same direction, and an SIW LWA with both high radiation efficiency and high gain can be expected.

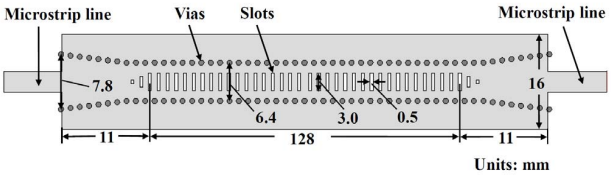

Fig. 3. Structure of the SIW LWA for fundamental wave radiation.

III. Design Procedure

The SIW LWAs are designed on the substrate of Rogers RO 3003 with thickness of $h = 1.524$ mm, permittivity of $\varepsilon_r = 3$ and loss tangent of 0.0013. The diameter of the vias of SIW is $d = 0.9$ mm, and the space between the adjacent vias is $s = 1.6$ mm. The SIWs for different elements are all working in TE_{10} mode, and the operating frequency is $f = 16$ GHz.

A. Structure of LWA for Fundamental Wave Radiation

The structure of SIW LWA for fundamental wave radiation is shown in Fig. 3. Radiation is generated by the periodic transverse slots etched on the top of the SIW, which interrupt the current flow along the SIW [9]. The dominant part of the LWA considered in this communication is 128 mm in length. In order to reduce the reflection, the width a_1 of the SIW at two ends is linearly tapered from 6.4 to 7.8 mm, and the slot length l_1 at the ends is also linearly tapered from 3 mm to 0, as shown in Fig. 3. The length of the tapered section is 11 mm, and the width of the slot is $w_1 = 0.5$ mm. The antenna is fed by a microstrip line with the impedance of 50 Ω.

The SIW can be taken as a conventional dielectric-filled rectangular waveguide with an effective width w_{eff}, which is approximately expressed by [6]

$$w_{eff} = a - 1.08 \times \frac{d^2}{s} + 0.1 \times \frac{d^2}{a}. \tag{8}$$

Therefore, the effective width of the SIW shown in Fig. 3 is $w_{\text{eff1}} = 5.8659$ mm. From (2), the equivalent dielectric constant ε_g of the leaky SIW is related to the permittivity ε_r, wavelength in free space λ_0, and the cut off wavelength of $TE_{10}\lambda_c'$. Since the difference between λ_c' and λ_c (the cut off wavelength of TE_{10} in closed waveguide) is not significant, so the equivalent dielectric constant ε_g is approximately expressed as

$$\varepsilon_g = \varepsilon_r - (\lambda_0/\lambda_c)^2. \tag{9}$$

According to the theory of rectangular waveguide, the cut off wavelength λ_c of TE_{10} in the closed SIW equals to twice of the effective width w_{eff}. Then, the equivalent dielectric constant ε_g for this SIW is about 0.45, which means the possibility that both the

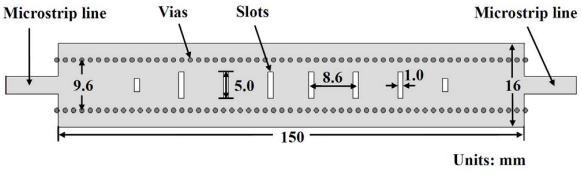

Fig. 4. Structure of the SIW LWA for −1th spatial harmonic radiation.

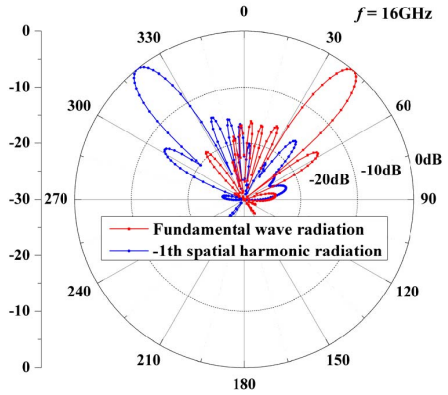

Fig. 5. Simulated radiation patterns (E-plane) of LWAs for fundamental wave radiation and −1th spatial harmonic radiation, respectively.

harmonics with positive and negative orders can leak away. From (5) and (3), we obtain the beam angle of the fundamental wave

$$\theta_0 = \sin^{-1}\sqrt{\varepsilon_g} = \frac{\beta}{k_0}. \tag{10}$$

For above-mentioned parameters, $\theta_0 = 42°$. In order to suppress the radiation from high-order harmonics and ensure that there is only one beam in space, according to (4) and (6), the period of the slots should be less than 7.85 mm, so it is chosen to $P_1 = 1.5$ mm in this communication.

B. Structure of LWA for −1th Spatial Harmonic Radiation

As stated earlier in Section II, the beam angle of the −1th spatial harmonic θ_{-1} should be equal to $-\theta_0$, and the equivalent dielectric constant should satisfy the condition of $\varepsilon_g \geq 1$, so that only the harmonics with negative order ($m < 0$) can leak away. Because this LWA is designed on the same substrate as that of fundamental wave radiation LWA, the effective width w_{eff} of this SIW must be carefully chosen to obtain a larger cut off wavelength λ_c, then ε_g can be larger than 1. To ensure the monoharmonic radiation, the range of slot period should follow formula (6).

Fig. 4 shows the geometry of the LWA that only allows −1th spatial harmonic to radiate. The SIW has a length of 150 mm, the width of two rows of vias is $a_2 = 9.6$ mm, and the effective width calculated from (8) is $w_{\text{eff2}} = 9.0617$ mm. To reduce the reflection, the slot length l_2 is also tapered from 5 mm to 0. The width of the slot of this antenna is $w_2 = 1$ mm, which is larger than that of the LWA for fundamental wave radiation to improve the radiation efficiency. Since the beam angle of the −1th spatial harmonic is known, $\theta_{-1} = \theta_0 = -42°$, the period of the slots, which can be calculated from (5) is $P_2 = 9.1$ mm. Because there are some approximations in ε_g calculation using (9), the realistic period for $\theta_{-1} = -42°$ may be a little different from 9.1 mm. Therefore, we adjusted the slot period, according to the full-wave simulation results, to make the radiation beam directions of the two antennas in opposition. The finally obtained slot period is $P_2 = 8.6$ mm, as shown in Fig. 4.

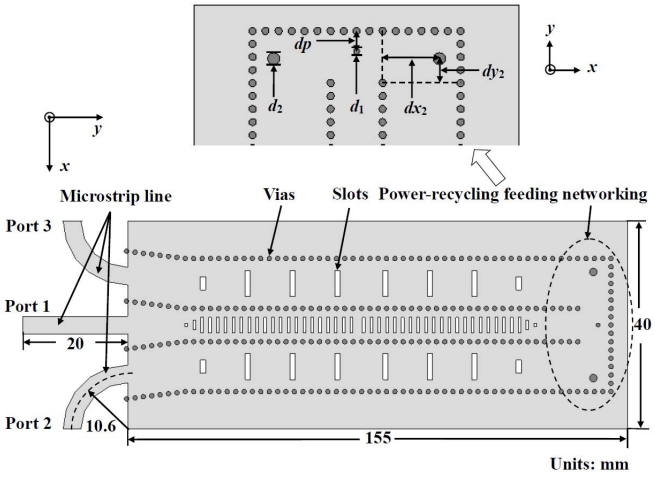

Fig. 6. Geometry of the proposed 3 × 1 SIW LWA array.

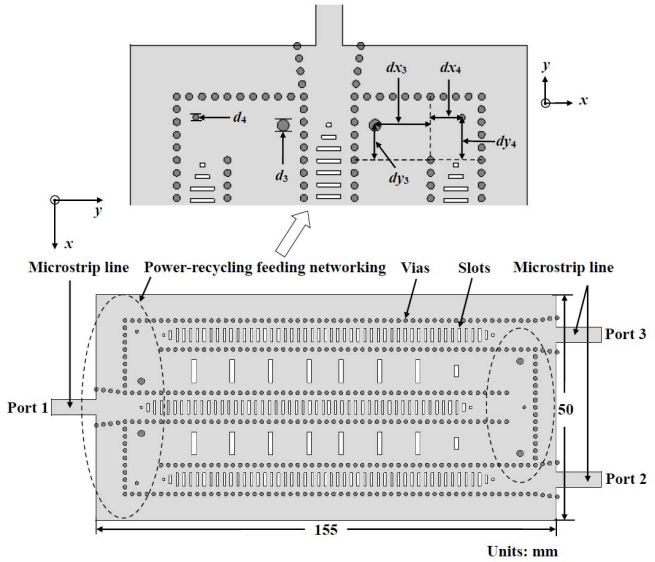

Fig. 7. Geometry of the proposed 5 × 1 SIW LWA array.

Fig. 5 shows the normalized radiation patterns of the two structures, as shown in Figs. 3 and 4, in E-plane ($\varphi = 90°$) at 16 GHz, illustrating that the radiation beam directions of these two antennas are in opposition. The beam angles of these two antennas are $\theta_0 = 40°$ and $\theta_{-1} = -40°$, respectively. Next, these kinds of antennas are used to construct a planar array with a novel power-recycling feeding network.

C. SIW Leaky-Wave Antenna Array

In order to construct the planar array as shown in Fig. 1, the SIW T-junction power divider must be used at the end of the central element, which is integrated on the same substrate to minimize the size of feeding network [10], [12]. A 3 × 1 SIW LWA array and a 5 × 1 SIW LWA array are considered in this section. Both of them are composed of three parts: three microstrip lines (one for feeding and two for rest power absorbing), leaky waveguide structures, and power-recycling feeding network, which consists of the T-junction power divider and several inductive posts.

The geometry of the proposed 3 × 1 SIW LWA array is shown in Fig. 6. Port 1 is connected to the source, and port 2 and port 3 are terminated with 50-Ω matching loads. The leaky waveguide

TABLE I

PARAMETERS OF THE FEEDING NETWORK OF 3 × 1 SIW LWA ARRAY (UNITS: mm)

d_1	dp	d_2	dx_2	dy_2
0.74	2.5	1.5	7.0	3.0

TABLE II

PARAMETERS OF THE FEEDING NETWORK OF 5 × 1 SIW LWA ARRAY (UNITS: mm)

d_3	d_4	dx_3	dy_3	dx_4	dy_4
1.5	0.74	7.0	4.6	4.0	5.6

structures are the same as those shown in Figs. 3 and 4. The power-recycling feeding network consists of one inductive post to divide the rest power at the output port of central element, and two symmetric inductive posts at the input ports of the neighboring elements to minimize the reflection of the SIW bends [11]. Table I shows the parameters of the power-recycling feeding network, which are optimized based on the structure of this SIW LWA array [13]. The geometry of the proposed 5 × 1 SIW LWA array is shown in Fig. 7. The whole structure of this antenna is similar to that of 3 × 1 array. The significant difference between them is in the part of leaky waveguide structure, in which two additional LWAs for fundamental wave radiation are added to improve the radiation efficiency further. Therefore, more inductive posts are adopted in the power-recycling feeding network to get a desirable return loss, as shown in Fig. 7. Table II shows the parameters of these new inductive posts. By optimizing the positions and diameters of these posts, the power-recycling feeding network can operate well as expected.

D. Simulation Results

Fig. 8 shows the normalized radiation patterns in E-plane ($\varphi = 90°$) and H-plane ($\theta = 40°$) for different array structures as shown in Figs. 3, 6, and 7 at 16 GHz. From Fig. 8(a), the main beams of these three antennas are almost pointing to the same direction at about 40°. From Fig. 8(b), we can see that the half-power beamwidth (HPBW) and the sidelobe level (SLL) in H-plane (passing through the maximum radiation direction) decrease as the number of array elements increasing. According to the basic principles of LWAs, the radiation beams of the fundamental radiation LWAs and −1th spatial harmonic radiation LWAs will strictly point to the same direction only at the frequency we design, which means that the proposed antenna arrays can only work in a certain frequency. However, owing to the finite beamwidth of the radiation beams, the antenna arrays can work in a certain frequency band without splitting of the radiation beams. Fig. 9 gives the frequency characteristics of the antenna arrays in terms of the radiation pattern. As we can see, with the frequency increasing or decreasing from 16 GHz, the performance of these two arrays get worse. The main beams will split into two lobes when the frequency increases or decreases by 200 MHz, which indicates that the frequency bandwidth of the array without beam splitting is about 400 MHz.

Table III gives the simulated performance of these LWAs. In order to accurately calculate the attenuation caused by radiation loss, the antenna is set to be made by perfect electric conductor and without dielectric loss, and the SIW is fed by wave port [14], which means that the radiation efficiency η_{RAD} can be approximately computed by $(1 - S_{11}^2 - S_{\text{out1}}^2)/(1 - S_{11}^2)$, as shown in Table III. It can be seen that the radiation efficiency and gain increase significantly when the array elements increase. The optimized matching structure also improves the performance of these LWAs. Compared with the LWA arrays proposed in [3], these arrays have more compact structures

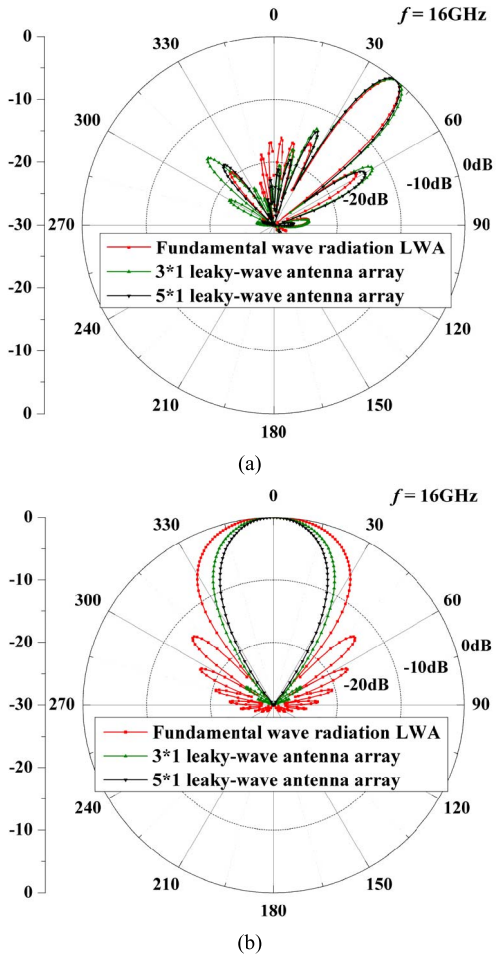

Fig. 8. Simulated radiation patterns of the LWAs in Figs. 3, 6, and 7 at 16 GHz. (a) E-plane. (b) H-plane (passing through the maximum radiation direction).

TABLE III

SIMULATED RESULTS OF THE SIW LWAS

Elements number	G (dB)	D (dB)	E-plane θ_m	H-plane HPBW	H-plane SLL (dB)	η_{RAD}
1	10.23	15.83	40°	48.1°	-13.3	28.89%
3	17.44	18.58	41°	35.4°	-24.9	89.60%
5	19.11	19.81	40°	30.2°	-29.8	94.12%

due to the application of SIW power divider and hybrid radiation of fundamental wave and −1th spatial harmonic of the SIW. On the other hand, our design has a more remarkable improvement of gain and radiation efficiency as given in Table III. The maximum radiation efficiency of the five-element LWA proposed in [3] is 78.29%, which is much lower in comparison with the five-element antenna array in this communication.

The transient electric field distributions above the top wall at $z = 1.6$ mm are plotted in Fig. 10 for the LWA arrays in Figs. 6 and 7. For constructive interference between adjacent waveguides, the length of each waveguide will be a crucial parameter, which should be an integral multiple of the wavelength in free space. From Fig. 10, we find that these two antenna arrays are well designed, so that the leaky waves radiating from the elements can be superposition in-phase in the desired direction.

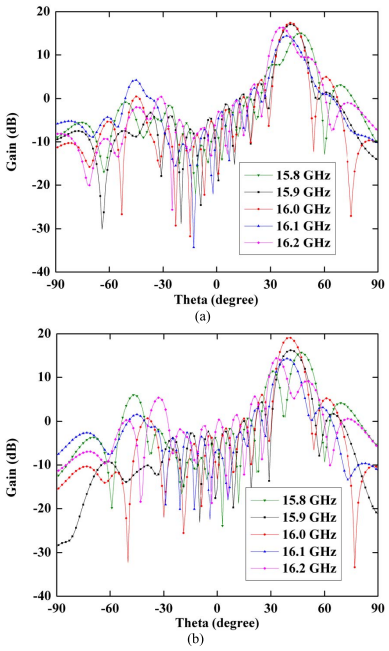

Fig. 9. Frequency characteristics of the antenna arrays in terms of the radiation pattern. (a) 3 × 1 SIW LWA array. (b) 5 × 1 SIW LWA array.

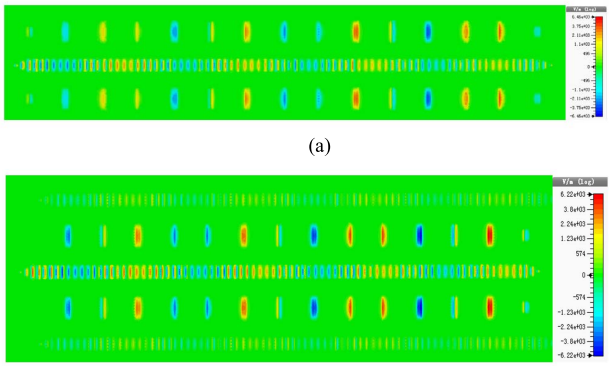

Fig. 10. Transient electric field distributions of the LWA arrays. (a) 3 × 1 SIW LWA array. (b) 5 × 1 SIW LWA array.

IV. Experimental Results

The proposed SIW LWAs were fabricated and measured. Fig. 11 shows the fabricated prototypes of the fundamental wave radiation SIW LWA, hybrid radiation of 3 × 1 SIW LWA array, and 5 × 1 SIW LWA array, from bottom to top.

A. S-Parameters

The measured S-parameters of the three antennas are depicted in Fig. 12, where Fig. 12(a) is for the insertion loss S_{21}^N and S_{31}^N and Fig. 12(b) is for the return loss S_{11}^N (elements number $N = 1, 3, 5$). As shown in Fig. 12(a), the insertion loss level at the operating frequency of 16 GHz decreases significantly as the number of array elements increasing from 1 to 5 as shown in Fig. 11, which indicates that less power will be absorbed by the matching loads, and therefore, more power has been dissipated for the proposed antenna arrays compared with the single LWA. From Fig. 12(b), it is found that the return loss is less than −10 dB within the passband of 15.5–18 GHz except for the 3 × 1 SIW LWA array at which the return loss increases slightly at 16.5 GHz or so. This is due to the reflection from the power-recycling feeding network, and the bend

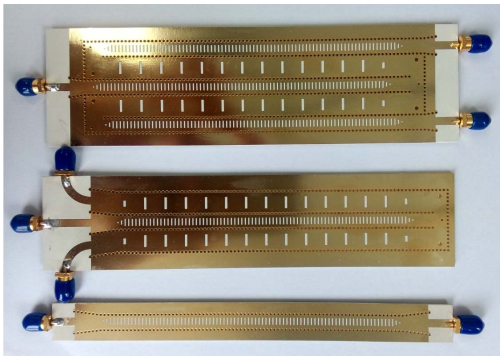

Fig. 11. Fabricated arrays with different sizes, fundamental wave radiation SIW LWA (bottom), 3 × 1 SIW LWA array (middle), and 5 × 1 SIW LWA array (top).

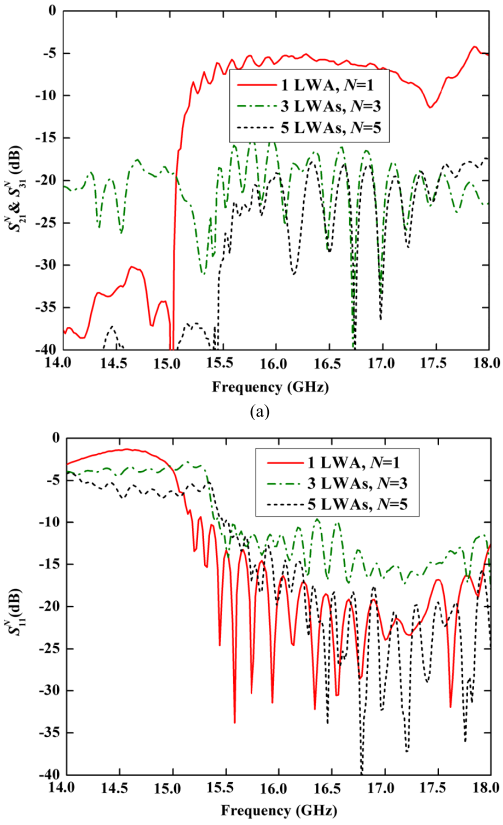

Fig. 12. Measured S-parameters of the three antennas with $N = 1$, 3, and 5 elements, respectively. (a) Insertion loss S_{21}^N and S_{31}^N. (b) Return loss S_{11}^N.

of the microstrip lines causing the mismatching between the sub-miniature-A connectors and the LWA.

B. Radiation Patterns

The measured normalized radiation patterns of the three prototypes are plotted in Fig. 13, and Fig. 13(a) shows those at the working frequency $f = 16$ GHz. It is observed that, in comparison with the full-wave simulation results in Fig. 8(a), there are some discrepancies between the simulation and measurement results. First, there are some slight shifts of beam directions of the antennas, and the SLLs are a little bit higher. Second, the main beams of 3 × 1 and 5 × 1 antenna arrays split into two lobes, illustrating the inconsistence of the beam directions of the fundamental wave radiation and the −1th spatial harmonic radiation of the fabricated antenna arrays. As we know, there are some manufacturing tolerances in the substrate parameters and some errors in the fabrication process, these all could affect the

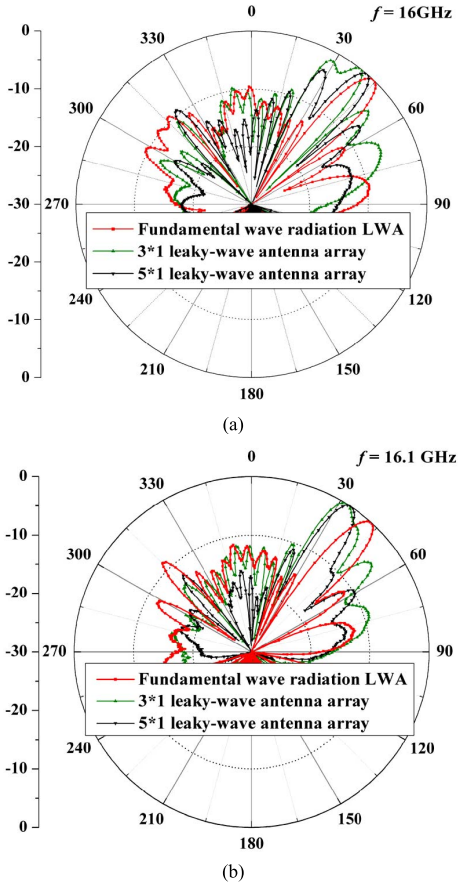

Fig. 13. Measured radiation patterns of the LWA prototypes in Fig. 11. (a) $f = 16$ GHz. (b) $f = 16.1$ GHz.

TABLE IV
MEASURED RESULTS OF THE SIW LWAS

Elements number	G (dB)	E-plane θ	H-plane HPBW	η_{DIS} ($1\text{-}S_{11}{}^2\text{-}S_{21}{}^2\text{-}S_{31}{}^2$)
1	11.16	42°	45.56°	73.83%
3	13.49	32°	28.59°	88.78%
5	15.96	34°	21.39°	96.26%

performances of a realistic antenna and make the measured results different from the simulated results of an ideally designed antenna. So, we check the beam directions of the fundamental wave and −1th spatial harmonic of the fabricated antenna arrays individually by screening one of them using copper strips, and found the fact that the beam splitting of the antennas is caused by the fabrication errors such as the accuracy of slots and posts position and size. However, as we know, the beam directions of the periodic structures are changing with the frequency, so we increase the frequency and the split beams become unsplit when $f = 16.1$ GHz, as shown in Fig. 13(b).

C. Gain and Radiation Efficiency

The measured radiation characteristics of the antennas at $f = 16.1$ GHz are summarized in Table IV. Compared with the simulated results shown in Table III, although the measured performance of these antennas are not very satisfactory and ideal as the simulated results due to the errors of fabrication and measurement, the gains and the efficiencies of the antennas, computed by the dissipated power ratio ($\eta_{\mathrm{DIS}} = 1-S_{11}^2-S_{21}^2-S_{31}^2$), increase as expected when the array elements increase from 1 to 5. This validates the proposed concept of this communication, that is, to improve the gain and efficiency of the LWA by using hybrid radiation of fundamental wave and −1th spatial harmonic.

V. CONCLUSION

A novel kind of the SIW LWA array with a power-recycling feeding network is proposed and validated in this communication. The antenna arrays exhibit high gain and high radiation efficiency, and decrease the HPBW and SLL in the H-plane in comparison with the single SIW LWA. Moreover, since the whole structure of the proposed antenna array constructs by two kinds of SIW LWAs on the same substrate and the novel power-recycling feeding network only consists of several metallic-vias on the planar substrate, which keeps it in a compact size, so it can be easily fabricated and integrated into microwave and millimeter-wave circuits.

REFERENCES

[1] A. Oliner and D. R. Jackson, "Leaky-wave antenna," in *Antenna Engineering Handbook*, J. L. Volakis, Ed. New York, NY, USA: McGraw-Hill, 2007.
[2] H. V. Nguyen, A. Parsa, and C. Caloz, "Power-recycling feedback system for maximization of leaky-wave antennas radiation efficiency," *IEEE Trans. Microw. Theory Techn.*, vol. 58, no. 7, pp. 1641–1650, Jul. 2010.
[3] H. V. Nguyen, S. Abielmona, and C. Caloz, "Highly efficient leaky-wave antenna array using a power-recycling series feeding network," *IEEE Antennas Wireless Propag. Lett.*, vol. 8, pp. 441–444, Mar. 2009.
[4] D. Deslandes and K. Wu, "Design consideration and performance analysis of substrate integrated waveguide components," in *Proc. 32nd Eur. Microw. Conf.*, Milan, Italy, Sep. 2002, pp. 1–4.
[5] Y. Cassivi, L. Perregrini, P. Arcioni, M. Bressan, K. Wu, and G. Conciauro, "Dispersion characteristics of substrate integrated rectangular waveguide," *IEEE Microw. Wireless Compon. Lett.*, vol. 12, no. 9, pp. 333–335, Sep. 2002.
[6] F. Xu and K. Wu, "Guided-wave and leakage characteristics of substrate integrated waveguide," *IEEE Trans. Microw. Theory Techn.*, vol. 53, no. 1, pp. 66–73, Jan. 2005.
[7] C. Zhang, J. Wang, M. Chen, and Z. Zhang, "Radiation characteristic of the leaky circular waveguide with periodic slots," *IEEE Antennas Wireless Propag. Lett.*, vol. 11, pp. 503–506, May 2012.
[8] J. Wang, Y. Geng, C. Zhang, and X. Huo, "Radiation characteristic of the periodic leaky wave structure and its application to leaky wave antenna design," in *Proc. Asia–Pacific Microw. Conf. (APMC)*, Nanjing, China, Dec. 2015, p. 1.
[9] J. Liu, D. R. Jackson, and Y. Long, "Substrate integrated waveguide (SIW) leaky-wave antenna with transverse slots," *IEEE Trans. Antennas Propag.*, vol. 60, no. 1, pp. 20–29, Jan. 2012.
[10] S. Germain, D. Deslandes, and K. Wu, "Development of substrate integrated waveguide power dividers," in *Proc. IEEE Can. Conf. Electr. Comput. Eng. (CCECE)*, May 2003, pp. 1921–1924.
[11] Z.-C. Hao, W. Hong, J.-X. Chen, X.-P. Chen, and K. Wu, "A novel feeding technique for antipodal linearly tapered slot antenna array," in *IEEE MTT-S Int. Microw. Symp. Dig.*, Jun. 2005, pp. 1641–1643.
[12] P. Chen *et al.*, "A multibeam antenna based on substrate integrated waveguide technology for MIMO wireless communications," *IEEE Trans. Antennas Propag.*, vol. 57, no. 6, pp. 1813–1821, Jun. 2009.
[13] Z. C. Hao, W. Hong, H. Li, H. Zhang, and K. Wu, "Multiway broadband substrate integrated waveguide (SIW) power divider," in *Proc. IEEE Antennas Propag. Soc. Int. Symp.*, Jul. 2005, pp. 639–642.
[14] Z. Li, J. Wang, M. Chen, and Z. Zhang, "New approach of radiation pattern control for leaky-wave antennas based on the effective radiation sections," *IEEE Trans. Antennas Propag.*, vol. 63, no. 7, pp. 2867–2878, Jul. 2015.
[15] J. B. Muldavin and G. M. Rebeiz, "Millimeter-wave tapered-slot antennas on synthesized low permittivity substrates," *IEEE Trans. Antennas Propag.*, vol. 47, no. 8, pp. 1276–1280, Aug. 1999.
[16] K. B. Ng, H. Wong, K. K. So, C. H. Chan, and K. M. Luk, "60 GHz plated through hole printed magneto-electric dipole antenna," *IEEE Trans. Antennas Propag.*, vol. 60, no. 7, pp. 3129–3136, Jul. 2012.
[17] D. Wang, K. B. Ng, C. H. Chan, and H. Wong, "A novel wideband differentially-fed higher-order mode millimeter-wave patch antenna," *IEEE Trans. Antennas Propag.*, vol. 63, no. 2, pp. 466–473, Feb. 2015.
[18] D. F. Filipovic, W. Y. Ali-Ahmad, and G. M. Rebeiz, "Millimeter-wave double-dipole antennas for high-gain integrated reflector illumination," *IEEE Trans. Microw. Theory Techn.*, vol. 40, no. 5, pp. 962–967, May 1992.